Pulse Radiolysis Study of the Reactions of Hydrogen Atoms in the Ionic Liquid Methyltributylammonium Bis[(trifluoromethyl)sulfonyl]imide

Jan Grodkowski[†] **and Pedatsur Neta***

Physical and Chemical Properties Division, National Institute of Standards and Technology, Gaithersburg, Maryland 20899

James F. Wishart

Chemistry Department, Brookhaven National Laboratory, Upton, New York 11973

Received: May 8, 2003; In Final Form: September 10, 2003

Reactions of hydrogen atoms with pyrene, phenanthrene, benzophenone, 2-propanol, and crotonic acid in the ionic liquid methyltributylammonium bis[(trifluoromethyl)sulfonyl]imide (R_4NNTf_2) were studied by pulse radiolysis. Radiolysis of the ionic liquid leads to formation of dry electrons and solvated electrons, which are scavenged by H_3O^+ to produce $H^•$ atoms. Hydrogen atoms react very rapidly with pyrene (3.8×10^9 L mol^{-1} s^{-1}) and phenanthrene (2.9×10^9 L mol^{-1} s^{-1}) to form H-adduct radicals with sharp absorption peaks at 405 and 395 nm, respectively. They also react with benzophenone to form ring adducts, but the reaction is much slower. By competition kinetics with pyrene, the rate constants for reactions of $H^•$ atoms with 2-PrOH and with crotonic acid were estimated to be $\approx 6 \times 10^7$ and 4.6×10^9 L mol^{-1} s^{-1}, respectively. All the rate constants, except for benzophenone, are similar to the values measured or estimated for the same reactions in aqueous solutions. The reactions with the aromatic hydrocarbons must be diffusion-controlled but are faster than diffusion-controlled reactions for solvated electrons in the same ionic liquid.

Introduction

Room-temperature ionic liquids[1] serve as good solvents for various thermal and electrochemical reactions, are nonvolatile and nonflammable, and have been proposed as solvents for green processing. To understand the effects of these solvents on rates of chemical reactions, the rate constants for several elementary reactions in ionic liquids have been studied[2] by the pulse radiolysis technique and compared with those in other solvents. In the ionic liquid methyltributylammonium bis[(trifluoromethyl)sulfonyl]imide (R_4NNTf_2) it was possible to observe the solvated electron and determine rate constants for its reactions with several aromatic compounds and with perchloric acid.[3] The solvated electron was observed to have a very broad absorption band peaking at 1400 nm with a molar absorption coefficient of 2.4×10^4 L mol^{-1} cm^{-1} and a radiolytic yield (G) of 0.6×10^{-7} mol J^{-1}. The rate constants for reaction of the solvated electron were determined for pyrene (1.7×10^8 L mol^{-1} s^{-1}), phenanthrene (1.3×10^8 L mol^{-1} s^{-1}), benzophenone (1.6×10^8 L mol^{-1} s^{-1}), and perchloric acid (6.2×10^7 L mol^{-1} s^{-1}). Dry (presolvated) electron capture by these solutes was also very efficient. The values of C_{37} (the concentration at which only 1/e, or 37%, of the electrons survive to be solvated) were 0.06−0.08 mol L^{-1} for the aromatic compounds and 0.2 mol L^{-1} for perchloric acid. In this study we utilize the reaction of the electron (both dry and solvated) with strong acids to produce hydrogen atoms and to determine the rate constants for reactions of $H^•$ atoms with several solutes. Such studies can be carried out with the aliphatic ionic liquid R_4NNTf_2 but not with ionic liquids that contain dialkylimidazolium or alkylpyridinium cations because these hererocyclic rings are strong scavengers for electrons and will prevent formation of $H^•$ atoms. In the present study we examine the reactions of $H^•$ atoms with the three aromatic compounds mentioned above, pyrene, phenanthrene, and benzophenone, and we utilize these results to determine the rate constants for 2-propanol and crotonic acid by competition kinetics.

Experimental Section[4]

Methyltributylammonium bis[(trifluoromethyl)sulfonyl]imide (R_4NNTf_2) was prepared as described before.[2b] Phenanthrene (Phen), benzophenone, crotonic acid, and triethylamine (TEA) were obtained from Aldrich, pyrene (Pyr) was from Eastman, and acetonitrile, methanol (MeOH), 2-propanol (2-PrOH), *tert*-butyl alcohol (*t*-BuOH), *p*-dioxane, and $HClO_4$ were from Mallinckrodt. Trifluoromethanesulfonic acid (HTFMS) was distilled prior to use. Water was purified with a Millipore Super-Q system.

Reaction kinetics and transient spectra were determined using the pulse radiolysis technique. Microsecond experiments were carried out at the National Institute of Standards and Technology with 0.1−1.5 μs pulses of 6 MeV electrons from a Varian linear accelerator; other details were as described before.[5] Nanosecond experiments were carried out at the Brookhaven National Laboratory Laser-Electron Accelerator Facility (LEAF). The LEAF RF photocathode electron accelerator was used to generate 8.7 MeV electron pulses of <200 ps duration. Narrow (10 nm) band-pass filters were used to select the analyzing light wavelength; 40 nm wide band-pass filters were used at wavelengths ≥1100 nm. Transient absorption signals were collected with FND-100 silicon (≤1050 nm) or GAP-500 InGaAs (≥900 nm) photodiodes, digitized with a Tektronix TDS-680B oscilloscope. Other details of these experiments were

---

[†] Present address: Institute of Nuclear Chemistry and Technology, Warsaw, Poland.

* Corresponding author.

10.1021/jp035265p CCC: $25.00

as described before,[3] and further details are provided in the Results. The dose per pulse was determined by thiocyanate dosimetry.[6] Unless stated otherwise, the measurements were performed at room temperature, 21 ± 2 °C. Rate constants and molar absorption coefficients are reported with their estimated standard uncertainties, taking into account the standard deviation of the experimental results and estimated uncertainties in the concentrations.

Results and Discussion

The absorption spectrum of the solvated electron formed in the radiolysis of neat R_4NNTf_2 has a peak at 1400 nm.[3] The rate constants for the reactions of e_{solv}^- with pyrene, phenanthrene, and benzophenone were found to be $(1.3-1.7) \times 10^8$ L mol^{-1} s^{-1},[3] which is assumed to be the diffusion-controlled limit in this viscous solvent. The rate constant for reaction of e_{solv}^- with perchloric acid was found to be slightly lower (6.2×10^7 L mol^{-1} s^{-1}). The latter reaction leads to formation of $H^\bullet$ atoms.

$$e_{solv}^- + H_3O^+ \rightarrow H^\bullet + H_2O \tag{1}$$

In addition to scavenging the solvated electron, the acid and the aromatic compounds can partly scavenge the "dry" electrons before they are solvated. It is assumed that scavenging of the dry electron by acid also produces $H^\bullet$ atoms (see below). In the present study we utilize both of these processes to produce $H^\bullet$ atoms and to determine the rate constants for their reactions with several solutes by pulse radiolysis.

Pyrene and Phenanthrene. Pulse irradiation of deoxygenated R_4NNTf_2 containing pyrene, but no acid, leads to rapid production of several species with optical absorption peaks at 405, 450, and 495 nm (Figure 1a). After 50 μs only the 405 nm peak remains and is more intense. The 495 nm peak is clearly ascribable to the pyrene radical anion[7,8] and its decay may be due to protonation[9] by traces of water or protons formed upon radiolysis or oxidation by other transient species (such as the positive "holes" produced by radiolysis or some of their fragmentation products).

$$e_{solv}^- + \text{Pyr} \rightarrow \text{Pyr}^{\bullet -} \tag{2}$$

$$\text{Pyr}^{\bullet -} + H^+ \rightarrow {}^\bullet\text{PyrH} \tag{3}$$

The 450 nm peak is partly due to the pyrene radical anion[7,8] and partly to the pyrene radical cation.[8,10] The latter species probably decays via hydroxylation by traces of water, reduction by other transient species, and reaction with neutral pyrene to form dimer cations. The 405 nm peak is ascribed to the pyrene H-adduct (i.e., the protonated pyrene radical anion), part of which is produced rapidly and part of which is produced during the protonation of the radical anion (reaction 3). In support of these assignments we found that the 495 nm peak ascribed to the pyrene radical anion was greatly diminished in the presence of other electron scavengers, such as O_2 or N_2O, but was not affected by 2-PrOH or triethylamine (TEA). The 450 nm peak, which is due in part to the radical cation, was diminished by TEA as well as by O_2.

These assignments were further supported by nanosecond pulse radiolysis experiments in ionic liquid solutions saturated with either Ar (Supporting Information, Figure 1S) or O_2 (≈2 mmol L^{-1}) (Supporting Information, Figures 2S−4S). The aromatic solutes were present in high enough concentration (up to 33 mmol L^{-1} pyrene and 40 mmol L^{-1} phenanthrene) to scavenge the same fraction of the dry electrons as in the absence of O_2.[3] The solutes can also capture some of the solvated electrons in competition with O_2. At the absorption maxima for the radical anions (490 nm for pyrene and 450 nm for phenanthrene) these species decayed through reaction with O_2 at observed rate constants of $(0.9-1.0) \times 10^7$ s^{-1}, independent of the aromatic solute concentration (Supporting Information, Figure 3S). In the case of pyrene at 450 nm (where both the radical anion and cation absorb) a significant fraction of absorbance attributable to the radical cation remained at 4 μs, long after the radical anion decayed (Supporting Information, Figure 2S as compared with 1S). Absorbance at 1410 nm (where neither the radical anion nor cation absorb, Supporting Information, Figure 4S)[11] was observed to increase over the microsecond time scale, and with pyrene concentration, indicating the equilibration of the radical cation $Py^{\bullet +}$ with the pyrene dimer cation[12] $(Py)_2^{\bullet +}$. For the 33 mM pyrene case, the rate constants for cation disappearance at 450 nm, $(9.0 \pm 0.6) \times 10^5$ s^{-1}, and dimer cation growth at 1410 nm, $(9.4 \pm 1.6) \times 10^5$ s^{-1}, agree within experimental error. At lower pyrene concentrations a reliable rate constant for growth at 1410 nm cannot be obtained because of the low signal/noise ratio.

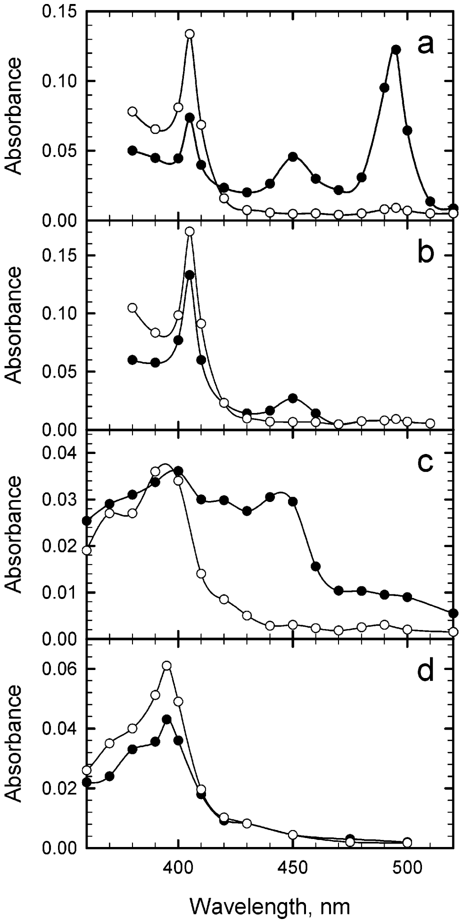

Figure 1. Transient optical absorption spectra monitored by pulse radiolysis of deoxygenated R_4NNTf_2 containing pyrene or phenanthrene: (a) 18 mmol L^{-1} pyrene; (b) 20 mmol L^{-1} pyrene with added 0.2 mol L^{-1} $HClO_4$; (c) 17 mmol L^{-1} phenanthrene; (d) 19 mmol L^{-1} phenanthrene with added 0.2 mol L^{-1} $HClO_4$. The spectra were recorded 1−2 μs (●) and 50−90 μs (○) after the pulse.

The spectrum recorded by pulse radiolysis of a deoxygenated pyrene solution containing 0.2 mol L^{-1} $HClO_4$ lacks the 495 nm absorption (Figure 1b). This result may be due either to a very rapid protonation of the anion radical by the acid (reaction 3) or reaction of the acid with the electron, which prevents formation of the pyrene radical anion. In either case, $\text{Pyr}^{\bullet -}$ is replaced by $^•$PyrH, and this is evident from the intense initial absorbance at 405 nm due to $^•$PyrH. Additional absorbance at 405 nm is formed more slowly due to reaction of $^•CF_3$ radicals with pyrene, as discussed before.[2c] In support of the assignment of the 405 nm peak to $^•$PyrH, we find that the H-adduct of pyrene, recorded in acetonitrile solutions containing 0.1 mol L^{-1} $HClO_4$, also exhibits a peak at 405 nm and the H-adduct of pyrenesulfonic acid, recorded in acidic aqueous solutions containing *t*-BuOH, has a peak at 415 nm. The H-adduct of pyrene in methanolic solutions was reported to have a peak at 400 nm.[13] Moreover, addition of propene to the acidic ionic liquid pyrene solution greatly diminishes the 405 nm peak. Because propene is a good H-atom scavenger but does not react with solvated electrons, this finding indicates that $^•$PyrH in acidic solutions is formed to a large extent by reaction of pyrene with $H^•$ atoms.

$$H^• + \text{Pyr} \rightarrow {}^•\text{PyrH} \qquad (4)$$

We can use the reported[3] rate constants for reactions 1 and 2 and C_{37} values for scavenging of dry electrons by pyrene and perchloric acid to calculate the distribution between reactions 3 and 4 as the source of $^•$PyrH. From the values of C_{37} for pyrene (0.063 mol L^{-1}) and for the acid (0.2 mol L^{-1}) and the concentrations in Figure 1b (0.02 mol L^{-1} pyrene and 0.2 mol L^{-1} acid) we calculate that 51% of the dry electrons are scavenged by the acid, presumably to form $H^•$ atoms, 22% are scavenged by pyrene, and 27% become solvated. From k_1 (6.2×10^7 L mol^{-1} s^{-1}) and k_2 (1.7×10^8 L mol^{-1} s^{-1}) we calculate that 78% of the solvated electrons react with the acid and 22% with pyrene. Thus in total, 72% of the electrons are converted to $H^•$ atoms and react with pyrene via reaction 4 whereas 28% of the electrons react directly with pyrene and form $^•$PyrH via reaction 3.

Parallel experiments with phenanthrene in R_4NNTf_2 gave very similar results (Figure 1c,d). The phenanthrene H-adduct ($^•$PhenH) exhibits an absorption peak at 395 nm whereas the radical anion ($\text{Phen}^{•-}$) has a peak at 445 nm and additional absorptions over most of the range recorded.[8,14] Calculation of the reaction distributions from the known rate constants and C_{37} values, as discussed above, shows that, under the conditions of Figure 1d, 78% of the electrons are converted to $H^•$ atoms and only 22% react with phenanthrene directly. The H-adduct of phenanthrene, with a peak at 395 nm, was also observed by pulse radiolysis in methanolic solutions, both neutral (formed by protonation of the radical anion) and acidic (formed also by reaction with $H^•$ atoms). The H-adduct in acidic acetonitrile solutions exhibited a peak at 375 nm.

The rate constants for reaction of $H^•$ atoms with pyrene and phenanthrene were determined by nanosecond pulse radiolysis using deoxygenated R_4NNTf_2 solutions that contained 0.2 mol L^{-1} acid and between 2 and 16 mmol L^{-1} aromatic hydrocarbon. Under these conditions, at least 75% of the electrons are converted into $H^•$ atoms and the reaction of $H^•$ atoms with the aromatic compound was monitored by following the buildup of absorption of $^•$PyrH at 405 nm or $^•$PhenH at 395 nm. In these experiments, a surprising result was obtained when $HClO_4$ was replaced with HTFMS. The absorption peak of the H-adduct was not observed. Because 70% perchloric acid contains a small amount of water whereas HTFMS was anhydrous, we examined whether water was necessary for production of $H^•$ atoms in the ionic liquid. Addition of 0.2 mol L^{-1} $HClO_4$ involves addition of 0.5 mol L^{-1} H_2O. Therefore, we added 0.5−2 mol L^{-1} water to the HTFMS ionic liquid solution and then, indeed, the absorption of the aromatic H-adduct was observed. Evidently, electrons in this ionic liquid react with H_3O^+ to produce $H^•$ atoms but some product other than the $H^•$ atom is formed from the reaction of the electron with HTFMS (or $HNTf_2$).

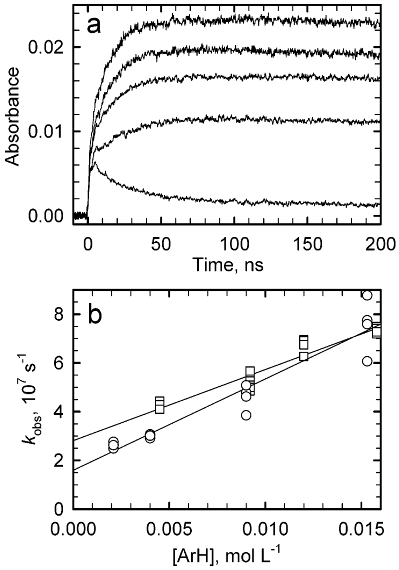

Figure 2. (a) Kinetic traces at 390 nm showing the formation of $^•$PhenH radicals by reaction of phenanthrene with $H^•$ atoms in deoxygenated R_4NNTf_2 solutions containing 0.5 mol L^{-1} HTFMS, 2 mol L^{-1} water, and (bottom to top) 0, 4.5, 9.2, 12.0, and 15.8 mmol L^{-1} phenanthrene. (b) First-order rate constants for formation of $^•$PhenH at 390 nm (squares) and $^•$PyrH at 400 nm (circles) as a function of the concentration of the aromatic hydrocarbon. The results for $^•$PhenH were obtained under the conditions of Figure 2a and the results for $^•$PyrH were obtained with 0.2 mol L^{-1} $HClO_4$, as described above.

TABLE 1: Rate Constants for Reactions of Hydrogen Atoms in the Ionic Liquid R_4NNTf_2

compound	rate constant (L mol^{-1} s^{-1})
pyrene	$(3.8 \pm 0.3) \times 10^9$
phenanthrene	$(2.9 \pm 0.3) \times 10^9$
benzophenone	$<1 \times 10^8$
crotonic acid	$(4.6 \pm 1.2) \times 10^9$
2-propanol	$(6 \pm 3) \times 10^7$

Sample traces for reaction of $H^•$ atoms with phenanthrene are shown in Figure 2a. The observed first-order rate constants calculated from such traces are in the range of $(2-8) \times 10^7$ s^{-1}. These values are similar to or higher than the first-order rate constant for reaction of solvated electrons with the acid at the 0.2−0.5 mol L^{-1} concentration used in these experiments ($(1-3) \times 10^7$ s^{-1}). Therefore, the observed reaction at the higher [ArH] values is due only to the $H^•$ atoms formed by reaction of the acid with dry electrons, which accounts for 60−90% of the total yield. The remaining dry electrons either react with the aromatic hydrocarbon to form the radical anion or become solvated. The reactions of the solvated electrons with both the acid and the aromatic compound are slower than the rate of formation of the H-adducts, at least at the higher [ArH] used, and are not observed on the time scale of Figure 2a. Their contribution was observed at longer times, but that kinetic step does not represent reaction 4, as it was limited by the rate of $H^•$ atom formation.

The first-order rate constants derived from the traces in Figure 2a and similar results for pyrene are plotted vs concentration in Figure 2b. The slopes of the lines yield second-order rate constants of $k(\text{H} + \text{pyrene}) = (3.8 \pm 0.3) \times 10^9$ L mol^{-1} s^{-1} and $k(\text{H} + \text{phenanthrene}) = (2.9 \pm 0.3) \times 10^9$ L mol^{-1} s^{-1} (Table 1). These values are higher by 1 order of magnitude than the rate constants for reactions of these compounds with solvated

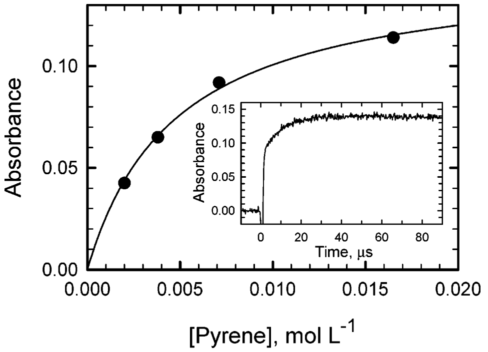

Figure 3. Absorbance recorded 1−2 µs after the pulse as a function of pyrene concentration. Inset: kinetic trace at 405 nm recorded by pulse radiolysis of R_4NNTf_2 solutions containing 7 mmol L^{-1} pyrene and 0.2 mol L^{-1} acid (see text).

electrons in the same ionic liquid. Both sets of values are considered to be diffusion-controlled, suggesting that diffusion of $H^•$ atoms in this solvent is faster that diffusion of solvated electrons. This finding is rationalized by the fact that $H^•$ atoms are small uncharged species that can diffuse through the ionic solvent faster than charged species.

Competition Kinetics. The results in Figure 1b,d show a rapid step of formation of the H-adduct followed by a slower step ascribed to reaction with $^•CF_3$ radicals.[2c] A sample kinetic trace on the microsecond time scale showing the two steps for pyrene at 405 nm is presented in Figure 3 (inset). The absorbance at the end of the fast step, as determined from extrapolation of the kinetic fit to the time of the pulse, increases with pyrene concentration, as shown in Figure 3. This plot shows that at a pyrene concentration of 0.02 mol L^{-1} there is nearly complete scavenging of the $H^•$ atoms by pyrene. The decrease in yield on decreasing concentration is due in part to competition between scavenging of $H^•$ atoms by pyrene and reactions of $H^•$ atoms with the solvent and with other radicals. If pyrene is to be used as a reference to determine relative rate constants for reactions of $H^•$ atoms with other compounds, one has to take into account the uncertainties stemming from the above competition. Moreover, one has to minimize the fraction of $^•$PyrH that is produced via reactions 2 and 3 by using lower concentrations of pyrene. As an optimal concentration for such competition we used 7 mmol L^{-1} pyrene, where the overall yield is decreased, but of this yield only 12% of $^•$PyrH are expected to be formed via the electron reaction and 88% via the $H^•$ atom reaction. Lowering the concentration below 7 mmol L^{-1} improves this reaction distribution but significantly decreases the overall yield.

Competition kinetic experiments were carried out with 2-PrOH by using a constant 7 mmol L^{-1} pyrene and varying concentrations of 2-PrOH between 0.3 and 1.2 mol L^{-1}. A plot of the reciprocal absorbance (1/*A*) vs the concentration ratio ([2-PrOH]/[pyrene]) is shown in Figure 4a. The competition equation can be given as

$$1/A = B + 1/A_0(k_{\mathrm{PrOH}}/k_{\mathrm{Pyr}})[\text{2-PrOH}]/[\text{pyrene}] \qquad (5)$$

where A_0 is the limiting absorbance at high pyrene concentrations in the absence of 2-PrOH, *A* is the absorbance measured at the experimental concentrations of pyrene and 2-PrOH, k_{Pyr} and k_{PrOH} are the second-order rate constants of pyrene and 2-PrOH, respectively, and *B* represents all the other competing reactions (with the solvent and with other radicals), assuming that their contribution is constant. The limiting value A_0 estimated from extrapolation of the results in Figure 3 is 0.15.

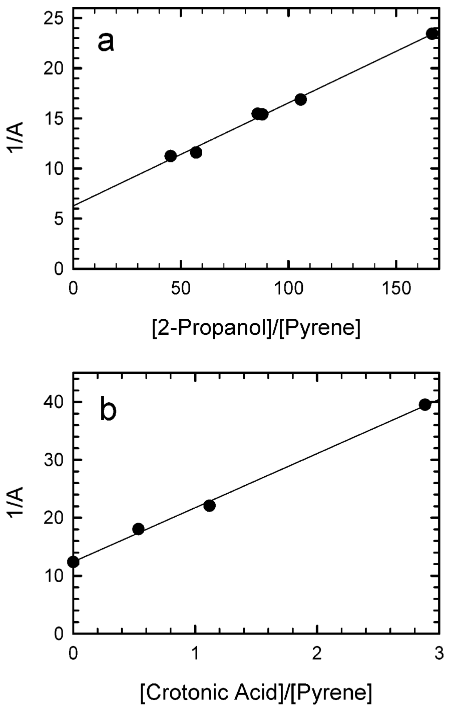

Figure 4. Competition plots showing the decrease in absorbance of $^•$PyrH at 405 nm with increasing 2-PrOH (a) or crotonic acid (b) concentration in deoxygenated R_4NNTf_2 solutions with added 0.2 mol L^{-1} $HClO_4$ (see text for details).

The slope of the line in Figure 4a is 0.10. By multiplying the slope with A_0, we obtain $k_{\mathrm{PrOH}}/k_{\mathrm{Pyr}} = 0.015$. From the absolute rate constants for pyrene ($k_4 = 3.8 \times 10^9$ L mol^{-1} s^{-1}) we calculate $k_6 = (6 \pm 3) \times 10^7$ L mol^{-1} s^{-1}.

$$H^• + (CH_3)_2CHOH \rightarrow H_2 + {}^•C(CH_3)_2OH \qquad (6)$$

The overall uncertainty in k_6 is estimated to be ±50% because, in addition to the uncertainties discussed above, the necessity to use large concentrations of 2-PrOH for the competition experiment introduces an additional uncertainty in the absorbance values due to the change in solvent composition.[15] The value of k_6 is similar to the rate constant for this reaction in aqueous solutions (7.4×10^7 L mol^{-1} s^{-1}).[16] This similarity is not surprising because the reaction involves neutral species and is not diffusion-controlled.

Competition kinetic experiments were carried out also with crotonic acid. The concentrations of crotonic acid required for the competition were of the same order of magnitude as those of pyrene so that the solvent composition was not changed to any appreciable extent. Moreover, to retain the same overall competition between the acid and the other solutes for the electrons, i.e., to maintain a constant H-atom yield, we kept the sum [pyrene] + [crotonic acid] constant (very close to 7 mmol L^{-1}) because both of these solutes are expected to react with electrons with similar rate constants. The plot of 1/*A* vs the concentration ratio (Figure 4b) gives a good straight line with a slope of 9.3. By multiplying this value with A_0, which is 0.13 for the dose used in these experiments, we derive $k_{\mathrm{Crotonic}}/k_{\mathrm{Pyrene}} = 1.2$. The uncertainty in this value is lower than that for the case of 2-PrOH and is estimated to be ± 25%. From $k_4 = 3.8 \times 10^9$ L mol^{-1} s^{-1} we calculate $k_7 = (4.6 \pm 1.2) \times 10^9$ L mol^{-1} s^{-1}. The reaction forms two isomeric H-adducts.

$$H^• + CH_3CH{=}CHCO_2H \rightarrow CH_3CH_2C^•HCO_2H + CH_3C^•HCH_2CO_2H \qquad (7)$$

The rate constant for reaction of H$^\bullet$ atoms with crotonic acid in aqueous solutions was not reported but other unsaturated acids, and hydrocarbons have rate constants that are in the same range as that determined for crotonic acid in the ionic liquid, indicating that addition of H$^\bullet$ to crotonic acid probably has similar rate constants in water and in the ionic liquid. It is interesting to note, however, that the rate constants for reactions of H$^\bullet$ atoms are higher than the rate constants for reactions of solvated electrons in the ionic liquid whereas in water they are generally slower.

Benzophenone. A disadvantage of the pyrene system is that the H-adduct and the protonated electron-adduct are effectively the same species, a mixture of isomers with possibly different isomer distributions but with the same overall optical absorption spectrum. In an attempt to better distinguish between the reactions of solvated electrons and hydrogen atoms we performed similar experiments with benzophenone. The radical anion of benzophenone protonates on the carbonyl group whereas addition of H$^\bullet$ atoms takes place mainly at the ring positions.

$$(C_6H_5)_2CO + e_{solv}^- \rightarrow [(C_6H_5)_2CO]^{\bullet -} \tag{8}$$

$$[(C_6H_5)_2CO]^{\bullet -} + H^+ = (C_6H_5)_2C^\bullet OH \tag{9}$$

$$(C_6H_5)_2CO + H^\bullet \rightarrow C_6H_5COC_6H_6^\bullet \tag{10}$$

In aqueous solutions, $[(C_6H_5)_2CO]^{\bullet -}$ has an absorption peak at 610 nm,[17−19] $(C_6H_5)_2C^\bullet OH$ at 545 nm,[18,19] and $C_6H_5COC_6H_6^\bullet$ at 390 nm.[19]

Pulse radiolysis of benzophenone in deoxygenated R_4NNTf_2 solutions produced a species with an absorption peak at ≈710 nm (Figure 5a), which converted within 40 μs to another species with a peak at 545 nm. The initial species must be the benzophenone radical anion. The spectrum of $[(C_6H_5)_2CO]^{\bullet -}$ has a peak at 610 nm in water,[17−19] but the peak shifts up to 650 nm in various alcohols and up to 700−750 nm in *p*-dioxane, cyclohexane, tetrahydrofuran, and triethylamine.[20] The peak at 710 nm found in the ionic liquid indicates that this solvent is somewhat similar to the latter four aprotic solvents in its solvatochromic effect on $[(C_6H_5)_2CO]^{\bullet -}$ and dissimilar to aqueous and alcohol solvents. The absorption peak of the protonated species, $(C_6H_5)_2C^\bullet OH$, on the other hand, is found near 540−550 nm in all of the above solvents.[18−20] Therefore, the peak observed at 545 nm in the ionic liquid is ascribed to $(C_6H_5)_2C^\bullet OH$, which is formed by protonation of the radical anion with the protons formed upon radiolysis.

To observe the H-adduct of benzophenone, we carried out experiments in acidic solutions. The spectrum has an intense absorption peak at 450 nm and a weaker absorbance at 545 nm (Figure 5a). The 450 nm peak is most likely due to the H-adduct of benzophenone because it was not observed in the absence of either the acid or the benzophenone. The spectrum of the benzophenone H-adduct was reported only in aqueous solutions and has a peak at 390 nm.[17,19] To confirm a solvent-induced shift for the absorption peak of this species, we monitored its spectrum in various solvents (Figure 5b). It was possible to observe the H-adduct only in solvents that do not react with H atoms rapidly: water (390 nm), MeOH (380 nm), *t*-BuOH (370 nm), acetonitrile (≤370 nm), and *p*-dioxane (440 nm). It is interesting to find that the absorption peak in the ionic liquid is again similar to that in dioxane, and this supports the assignment of the H-adduct.

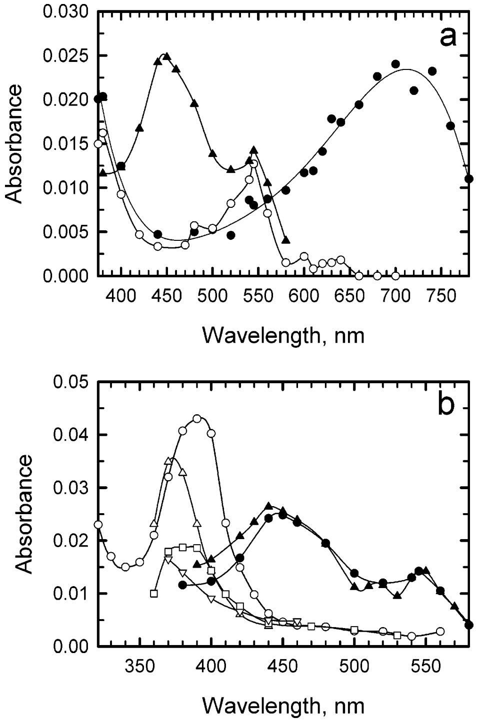

Figure 5. (a) Transient optical absorption spectra monitored by pulse radiolysis of deoxygenated R_4NNTf_2 containing benzophenone (BP). Solution a: 19 mmol L^{-1} BP, spectra recorded 1 μs (solid circles) and 40 μs (open circles) after the pulse;. Solution b: 26 mmol L^{-1} BP with added 0.1 mol L^{-1} $HClO_4$, 1 μs (solid triangles) after the pulse. (b) Absorption spectra for the benzophenone H-adduct in various solvents: (solid circles) R_4NNTf_2, 26 mmol L^{-1} BP, and 0.1 mol L^{-1} $HClO_4$; (solid triangles) *p*-dioxane, 82 mmol L^{-1} BP, and 3 mol L^{-1} $HClO_4$; (circles) water, 1 mol L^{-1} t-BuOH, 0.6 mmol L^{-1} BP, and 0.1 mol L^{-1} $HClO_4$ (the same spectrum was found with added 2.9 mol L^{-1} $NaClO_4$); (open triangles) *t*-BuOH, 10 mmol L^{-1} BP, and 0.1 mol L^{-1} $HClO_4$; (open squares) MeOH, 10 mmol L^{-1} BP, and 3 mol L^{-1} $HClO_4$; (inverted triangles) MeCN, 10 mmol L^{-1} BP, and 0.1 mol L^{-1} $HClO_4$.

Nanosecond pulse radiolysis experiments to determine the rate constant for reaction of H$^\bullet$ atoms with benzophenone (reaction 10) showed formation of absorption at 440 nm with rate constants (≈6×10^6 s^{-1}) that were practically independent of benzophenone concentration and lower than the intercepts in Figure 2b. This finding leads to the conclusion that the reaction is much slower than that observed for pyrene and phenanthrene, probably $k_{10} < 1 \times 10^8$ L mol^{-1} s^{-1}. The rate constant could not be determined by increasing the concentration of benzophenone because at the high concentrations required to observe this reaction most of the dry electrons are scavenged by benzophenone rather than by the acid. With 0.2 mol L^{-1} acid and the highest benzophenone concentration used in these experiments, 0.09 mol L^{-1}, 50% of the dry electrons are scavenged by benzophenone and only 41% by the acid. To determine a second-order rate constant that is smaller than 1×10^8 L mol^{-1} s^{-1} when the intercept is ≈6×10^6 s^{-1}, it is necessary to use benzophenone concentrations higher than 0.2 mol L^{-1}, and at this concentration 96% of the dry electrons will be scavenged by benzophenone. Therefore, we can only conclude that $k_{10} \ll k_4$. In the microsecond pulse radiolysis experiments of Figure 5a the spectrum of the H-adduct was recorded with 0.026 mol L^{-1} benzophenone and 0.1 mol L^{-1} perchloric acid. At these concentrations 32% of the dry electrons are scavenged by the acid, 28% by benzophenone, and 40% become solvated. Of the solvated electrons 60% react with the acid and 40% with benzophenone. Thus a total of 56% of the electrons are converted into $H^•$ atoms, some of which react with benzophenone and the rest decay via other processes. This partial yield of H-adducts is observed in Figure 5a but its formation involves complex kinetics.

Conclusion

To measure the reactivity of $H^•$ atoms with aromatic solutes in ionic liquids, it is first necessary to understand the reactivity of presolvated, “dry” electrons with the substrates. A prime example is benzophenone, where dry electron capture is so efficient that it obscures the observation of the relatively slow $H^•$ atom reaction. Reactions of $H^•$ atoms with pyrene and phenanthrene are significantly faster ($k_{\text{pyrene}} = 3.8 \times 10^9$ L mol^{-1} s^{-1}, $k_{\text{phenanthrene}} = 2.9 \times 10^9$ L mol^{-1} s^{-1}) and readily observed, even in the presence of dry electron scavenging. It is not clear why the rate constant for benzophenone should be so much slower, because the rate constants in water for $H^•$ atom reactions with benzophenone and other aromatic compounds are generally on the order of 10^9 L mol^{-1} s^{-1}. The present finding suggests that further investigation of the chemistry of benzophenone in acidic ionic liquid media is warranted.

In earlier work, a leveling effect was observed for the reactions of several aromatic solutes with the solvated electron, implying that the diffusion-limited rate constant was $\approx 2 \times 10^8$ L mol^{-1} s^{-1}. The rate constants for reactions of pyrene and phenanthrene with $H^•$ atoms are 10 times higher than for the corresponding solvated electron reactions, implying that the diffusion-limited rate constant for $H^•$ atom reactions is higher by an order of magnitude. The trend in this ionic liquid is opposite to that observed in water. It is possible that a small, neutral species such as $H^•$ can move easily between voids within the ionic liquid,[3] whereas the solvated electron, being a charged species, must interact with the ionic charges of the medium to diffuse.

Acknowledgment. The work performed at Brookhaven National Laboratory was funded under contract DE-AC02-98CH10886 with the U.S. Department of Energy and supported by its Division of Chemical Sciences, Office of Science.

Supporting Information Available: Transient absorption spectra. This material is available free of charge via the Internet at http://pubs.acs.org.

References and Notes

(1) Welton, T. *Chem. Rev.* **1999**, *99*, 2071. Wasserscheid, P.; Keim, W. *Angew. Chem., Int. Ed.* **2000**, *39*, 3772. Earle, M. J.; Seddon, K. R. *Pure Appl. Chem.* **2000**, *70*, 1391. Brennecke, J. F.; Maginn, E. J. *AIChE J.* **2001**, *47*, 2384.

(2) (a) Behar, D.; Gonzalez, C.; Neta, P. *J. Phys. Chem. A* **2001**, *105*, 7607. (b) Behar, D.; Neta, P.; Schultheisz, C. *J. Phys. Chem. A* **2002**, *106*, 3139. (c) Grodkowski, J.; Neta, P. *J. Phys. Chem. A* **2002**, *106*, 5468. (d) Grodkowski, J.; Neta, P. *J. Phys. Chem. A* **2002**, *106*, 9030. (e) Grodkowski, J.; Neta, P. *J. Phys. Chem. A* **2002**, *106*, 11130.

(3) Wishart, J. F.; Neta, P. *J. Phys. Chem. B* **2003**, *107*, 7261.

(4) The mention of commercial equipment or material does not imply recognition or endorsement by the National Institute of Standards and Technology, nor does it imply that the material or equipment identified are necessarily the best available for the purpose.

(5) Grodkowski, J.; Neta, P. *J. Phys. Chem. A* **2000**, *104*, 4475.

(6) Schuler, R. H.; Patterson, L. K.; Janata, E. *J. Phys. Chem.* **1980**, *84*, 2088.

(7) Arai, S.; Grev, D. A.; Dorfman, L. M. *J. Chem. Phys.* **1967**, *46*, 2572. Hayon, E. *J. Chem. Phys.* **1970**, *53*, 2353.

(8) Shida, T.; Iwata, S. *J. Am. Chem. Soc.* **1973**, *95*, 3473. Shida, T. *Electronic Absorption Spectra of Radical Ions*; Elsevier Science Publishers B.V.: Amsterdam, 1988.

(9) Arai, S.; Tremba, E. L.; Brandon, J. R.; Dorfman, L. M. *Can. J. Chem.* **1967**, *45*, 1119. Levanon, H.; Neta, P.; Trozzolo, A. M. *Chem. Phys. Lett.* **1978**, *54*, 181.

(10) Badger, B.; Brocklehurst, B. *Trans. Faraday Soc.* **1969**, *65*, 2588. Richards, J. T.; West, G.; Thomas, J. K. *J. Phys. Chem.* **1970**, *74*, 4137.

(11) Shaede, E. A.; Kurihara, H.; Dorfman, L. M. *Int. J. Radiat. Phys. Chem.* **1974**, *6*, 47−54.

(12) Kira, A.; Imamura, M *J. Phys. Chem.* **1979**, *83*, 2267−2273.

(13) Zhang, G.; Thomas, J. K. *J. Phys. Chem.* **1994**, *98*, 11714.

(14) Paul, D. E.; Lipkin, D.; Weissman, S. I. *J. Am. Chem. Soc.* **1956**, *78*, 116. Balk, P.; Hoijtink, G. J.; Schreurs, J. W. H. *Recl. Trav. Chim.* **1957**, *76*, 813.

(15) The intercept in Figure 4a is smaller than that in Figure 4b, indicating a higher yield in the presence of ≈0.3 mol L^{-1} 2-PrOH as compared with several mmol L^{-1} crotonic acid. Such an increase in yield by 2-PrOH has been observed before[2c] and was ascribed to an increase in the cage escape yield of electrons by scavenging of positive holes and other radicals. This effect is pronounced at the high concentrations used with 2-PrOH, which is a good positive hole scavenger, but the effect is small at the low concentrations used with crotonic acid.

(16) Buxton, G. V.; Greenstock, C. L.; Helman, W. P.; Ross, A. B. *J. Phys. Chem. Ref. Data* **1988**, *17*, 513. NDRL/NIST Solution Kinetics Database, NIST Standard Reference Database 40, 1995. http://kinetics.nist.gov/solution/index.php

(17) Adams, G. E.; Baxendale, J. H.; Boag, J. W. *Proc. R. Soc. (London) A* **1964**, *277*, 549.

(18) Adams, G. E.; Willson, R. L. *J. Chem. Soc., Faraday Trans. 1* **1973**, *69*, 719.

(19) Hayon, E.; Ibata, T.; Lichtin, N. N.; Simic, M. *J. Phys. Chem.* **1972**, *76*, 2072.

(20) Dainton, F. S.; Kemp, T. J.; Salmon, G. A.; Keene, J. P. *Nature* **1964**, *203*, 1050. Scholes, G.; Simic, M.; Adams, G. E.; Boag, J. W.; Michael, B. D. *Nature* **1964**, *204*, 1187. Keene, J. P.; Kemp, T. J.; Salmon, G. A. *Proc. R. Soc. (London) A* **1965**, *287*, 494. Keene, J. P.; Land, E. J.; Swallow, A. J. *J. Am. Chem. Soc.* **1965**, *87*, 5284. Baxendale, J. H.; Fielden, E. M.; Keene, J. P. *Science* **1965**, *148*, 637. Beaumond, D.; Rodgers, M. A. J. *Trans. Faraday Soc.* **1969**, *65*, 2973.